NASA Technical Memorandum 83565

Characteristic Morphological and Frictional Changes in Sputtered MoS_2 Films

(NASA-TM-83565) CHARACTERISTIC MORPHOLOGICAL AND FRICT...NAL CHANGES IN SPUTTERED MoS/SUB 2 FILMS (NASA) 16 p HC A02/MF A01 CSCL 20L

N84-16380

Unclas
G3/31 18154

Talivaldis Spalvins
Lewis Research Center
Cleveland, Ohio

Prepared for the
International Solid Lubricants Conference
sponsored by the American Society of Lubrication Engineers
Denver, Colorado, August 6-9, 1984

NASA

CHARACTERISTIC MORPHOLOGICAL AND FRICTIONAL CHANGES IN SPUTTERED MoS_2 FILMS

Talivaldis Spalvins

National Aeronautics and Space Administration
Lewis Research Center
Cleveland, Ohio 44135

Abstract

Three microstructural growth stages of sputtered MoS_2 films were identified with respect to film thickness: (1) ridge formation during nucleation, (2) an equiaxed transition zone, and (3) a columnar-fiber-like structure. Each of these growth stages are characterized in terms of microcrystallite size, shape, and orientation. The effective lubricating film thickness is established in terms of the microstructural growth stages during sliding experiments. The film has a tendency to break up within the columnar zone. Actual lubrication is performed by the remaining film which is 0.18 to 0.22 μm thick. Also a visual screening is proposed to evaluate the integrity of the as-sputtered MoS_2 film. The lubricating properties are identified with respect to optical changes before and after wiping. The orientation of the microcrystallites are responsible for the optical reflective changes observed.

INTRODUCTION

It is generally established that the lubricating properties and the endurance lives of sputtered MoS_2 films are directly influenced by the selected sputtering process variables and substrate chemistry, temperature, and topography, which in turn affect the crystalline-amorphous, morphological growth and compositional structures of the film (1-6). Therefore, the structural and compositional characterization of sputtered MoS_2 films from the nano-micro-macrostructural levels is of prime importance to understand the changes in the tribological behavior. Microstructural and compositional changes in the sputtered films are reflected in the coefficient of friction, either by a low (<0.04) or a high (>0.4) coefficient of friction during the lubrication process. To achieve an effective MoS_2 lubrication two requirements have to be met: (1) a low crystalline slip during shearing and (2) strong film/substrate adherence.

It is well established that sputtered MoS_2 films deposited at cryogenic substrate temperatures form an amorphous structure thus destroying the crystallinity necessary for easy slip. Therefore it is essential to preserve the hexagonal layered crystal structure. The amorphous films during friction studies act as abrasives and display very high coefficients of friction. Sputtered MoS_2 films generally have strong adherence to most metallic surfaces with the presently known exceptions being copper and silver and their alloys (7). These two metals are highly reactive with the activated free sulphur during the sputtering process, thus forming sulphur compounds which have the tendency to flake off the surface.

The objective of this paper is to establish the microstructural growth stages at ambient substrate temperatures in the thickness range of 0.02 to 1.2 μm and microstructurally characterize each growth stage and establish an effective film thickness during friction studies. Further, a visual screening (optical reflectivity) of the as-sputtered films before and after rubbing, in terms of microcrystallite orientation, is proposed for identifying the integrity of the film as a lubricant.

APPARATUS AND PROCEDURE

The sputtering apparatus used in this investigation, an rf-diode system with a superimposed dc bias, is described in Ref. 8. The planar MoS_2 sputtering target was 12.7 cm in diameter and 0.6 cm wide and had a 75-percent bulk density. Before sputter deposition the target was cleaned and outgassed by presputtering until the pressure stabilized. The sputtering argon pressure was 2.7 mPa, with a power density of 3.5 W/cm^2, and the average deposition rate was 0.025 μm/min for a target-to-substrate distance of 2.5 cm. The substrate temperatures were between 50° and 125° C and depended directly on the sputtering time, namely, 50° C for a sputter duration of 2 min and 125° C for 60 min. The substrates used were nickel and aluminum foils, microscopic glass slides, and 440C stainless-steel disks (6.25 cm in dia. and 1.25 cm thick). The temperature was monitored by a Chromel-Alumel thermocouple embedded in the disk, with the foils and microscopic slides mounted on the disk surface. The substrate surfaces were sputter cleaned before sputter deposition. The growth patterns and film textures in the 0.02 to 1.2-μm range were examined by transmission electron microscopy (TEM), electron diffraction (ED), and scanning electron microscopy (SEM). The chemical composition was analyzed by Auger electron spectroscopy (AES).

CRYSTAL STRUCTURE OF MoS_2

MoS_2 has an highly anistropic hexagonal crystal layered lattice structure, which consists of a layer of Mo atoms sandwiched between two layers of S atoms as shown in Fig. 1. Each atom of Mo is surrounded at equal distances by six S atoms placed at the corners of a triangular prism. The distance between the layers of Mo and

S atoms is 1.54 Å and the actual thickness of the lamella is 3.08 Å. The bonds between the Mo and S atoms are covalent and therefore strongly attractive. But the inter-lamellar attractions between the S layers are very weak, consisting only of Van der Waals forces. As a result MoS_2 crystals easily cleave along the Van der Waals gap. Since no covalent bonds are broken by such a cleavage, the exposed basal plane surfaces are relatively inert (9). The edge surfaces which are parallel to the c-axis, have Mo atoms which are coordinatively unsaturated. The basic feature which controls and determines the exact crystal structure is the chemical bonding which in turn is governed by complex electron interactions between the neighboring atoms. Adsorption studies have indicated that the edge surface sites are more active toward adsorption and reaction, especially exhibiting a preferrential affinity for polar compounds (9). This anisotropic crystallographic adsorption and reaction is of great importance when MoS_2 films are stored under atmospheric conditions (10).

MICROMORPHOLOGICAL GROWTH TRANSFORMATION STAGES

The micromorphological growth patterns of sputtered MoS_2 films in the thickness range of about 20 to 2000 nm were characterized by TEM, ED, and SEM. Three distinct micromorphological stages on the basis of film thickness were identified: (1) ridge formation during nucleation, (2) an equiaxed transformation zone, and (3) a columnar-fiber structure. Each of these structures were further characterized as to microcrystallite size, shape, and orientation.

Ridge formation. - The first transformation stage of a ultra thin (0.02 to 0.05 μm) sputtered MoS_2 film has the characteristic ridge formation as shown in Fig. 2. At ambient or elevated substrate temperatures the nucleation stage is a thermally activated diffusion process in which the sputtered atoms have some movement. If the temperature is high enough, larger atomic motion leads to the formation of long-range order and the microcrystallite size increases with increasing temperature. At elevated substrate temperatures (320° C) the diffraction rings become sharp as shown in Fig. 2 due to the larger microcrystallite size which is in the range 11 to 14 nm. As a result, the five diffraction rings can be accurately identified that correspond to the (100), (110), (200), (210), and (300) planes. MoS_2 films sputtered at ambient temperatures (>40° C) produce smaller microcrystallites, generally in the range 4.5 to 6.0 nm, and the corresponding diffractograms display more diffuse ring pattern. As previously determined (11) MoS_2 films sputtered on cryogenically cooled substrates where the sputtered particles are quench condensed form an amorphous structure. This structure has a short range atomic order without a crystalline atomic periodicity. The particle size is normally less than 2 nm and the atomic order starts to break down. The amorphous state is believed to resemble somewhat the liquid or glassy state. The amorphous state, due to the absence of crystallinity, does not display any lubricating properties. The range of microcrystallite diameter of sputtered MoS_2 films is plotted as a function of substrate temperature in Fig. 3.

The formation of the black needle type ridges is explained in terms of orientation and curling or rolling-up effects as observed by stereomicroscopy. These hexagonal microplatelets with their basal planes perpendicular to the substrate or the platelet roll-ups are responsible for the black ridge formations. The microplatelets with basal planes parallel to the substrate display the gray areas. Basically, the as sputtered MoS_2 films have the microplatelets oriented perpendicular and parallel to the substrate with a small portion of these microplatelets in a curled or rolled-up position. If this ridge type structure comes in stationary contact or in a rubbing condition with another surface a complete structural change takes place. The characteristic microstructural change is shown by TEM micrographs and diffractograms in Fig. 4 for a sputtered MoS_2 film at ambient temperatures. The ridge type micromorphology changed into spheroidal like particles. These spheroidal microcrystallites have a tendency to form agglomerations with widely assorted powderpuff like structures.

Equiaxed and columnar-fiber structure. As the film thickness increases to over 0.08 μm, the ridge type structure transforms into an equiaxed, dense transition zone, before it grows into a columnar-fiber like structural network as shown in the SEM micrographs of Fig. 5. The columnar-fiber structure consists of vertical platelets about 0.25 μm in diameter that are clearly aligned perpendicular to the substrate. The diameter of the tapered platelets and the density of the array of the microcolumns changes with the surface smoothness. The columnar platelets are separated longitudinally by low density regions (microvoids), therefore these regions have a high level of residual stress. However, films on smooth microscopic slides show a dense array of microcolumns. The morophological growth zones are schematically shown in Fig. 6.

EFFECTIVE FILM THICKNESS

In solid film lubrication where thin soft metallic films (Au, Ag, Pb) are ion plated or sputtered, the film thickness has a very pronounced effect on the coefficient of friction (12). Essentially, the coefficient of friction reaches a minimum value at an effective or critical film thickness as shown in Fig. 7. Based on the friction coefficient, the variation of film thickness can be divided into two regions, the ultra thin and the thin film region with an effective or critical film thickness in the 200 nm range at which the friction coefficient reaches the minimum value of about 0.1. At the effective film thickness the actual lubrication is performed. It should be realized, that in thin film lubrication the relationship between the critical film thickness and the minimum

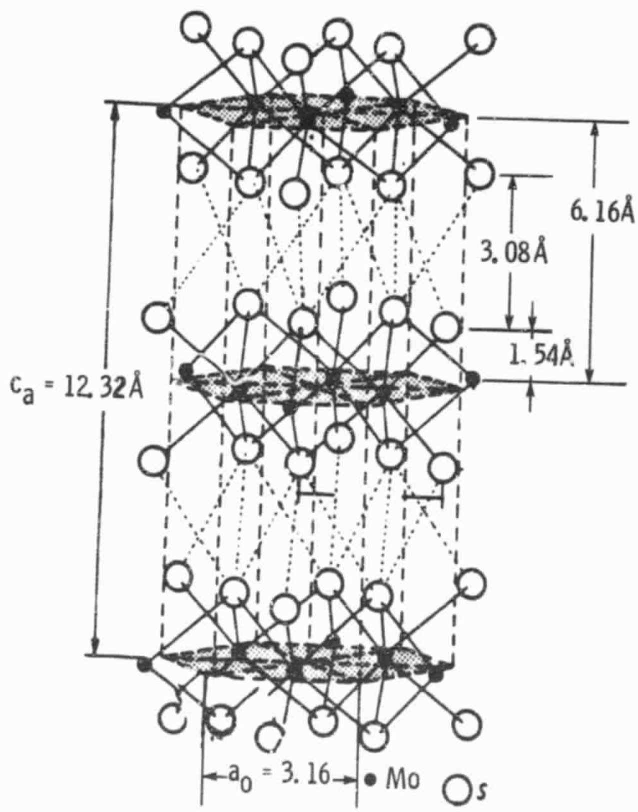

Figure 1. - Structure of MoS_2.

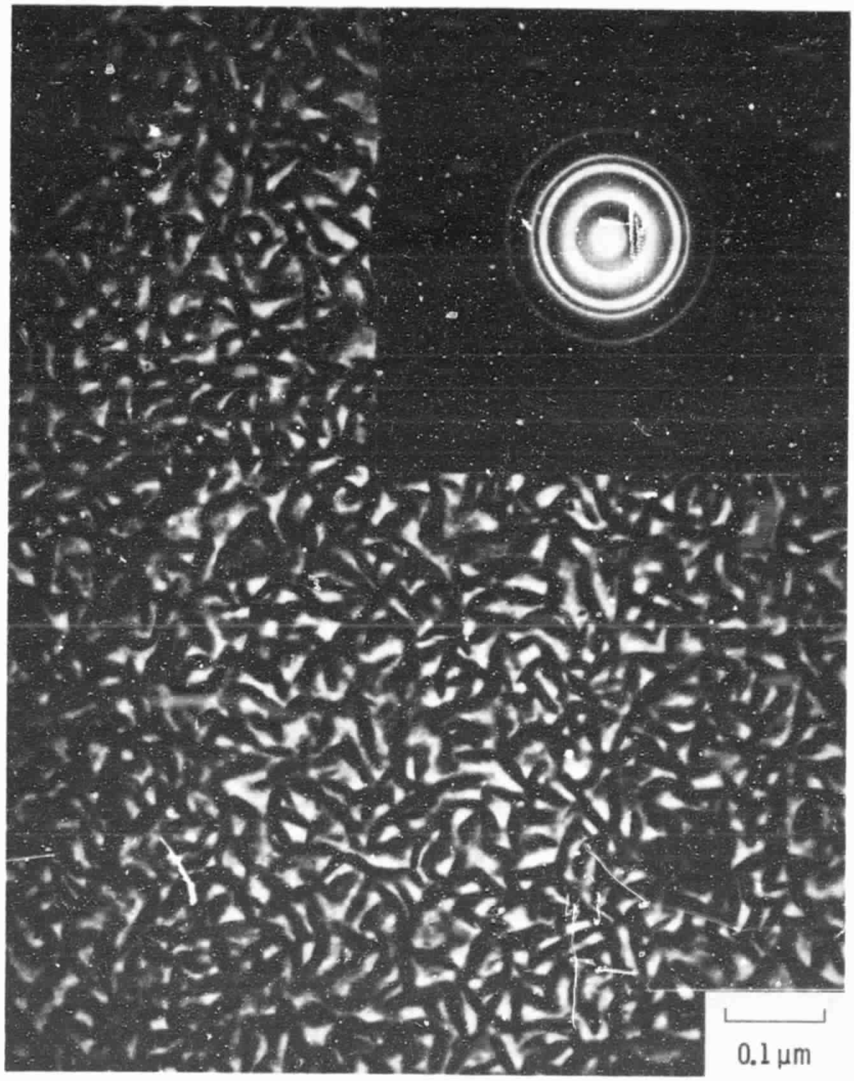

Figure 2. - Electron transmission micrograph and diffractogram of sputtered MoS_2 on aluminum.

ORIGINAL PAGE IS
OF POOR QUALITY

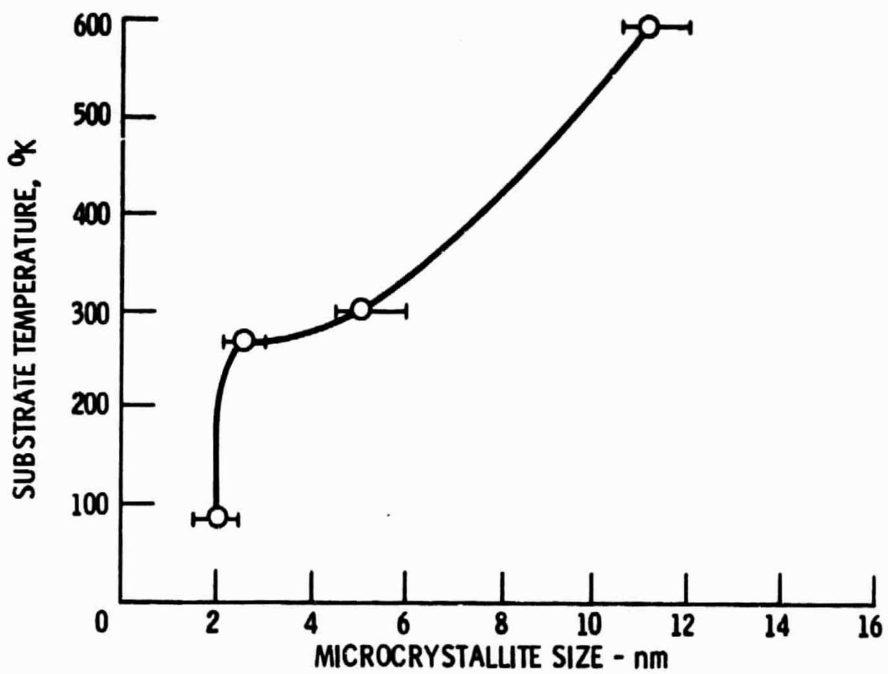

Figure 3. - The change in microcrystallite size as a function of temperature.

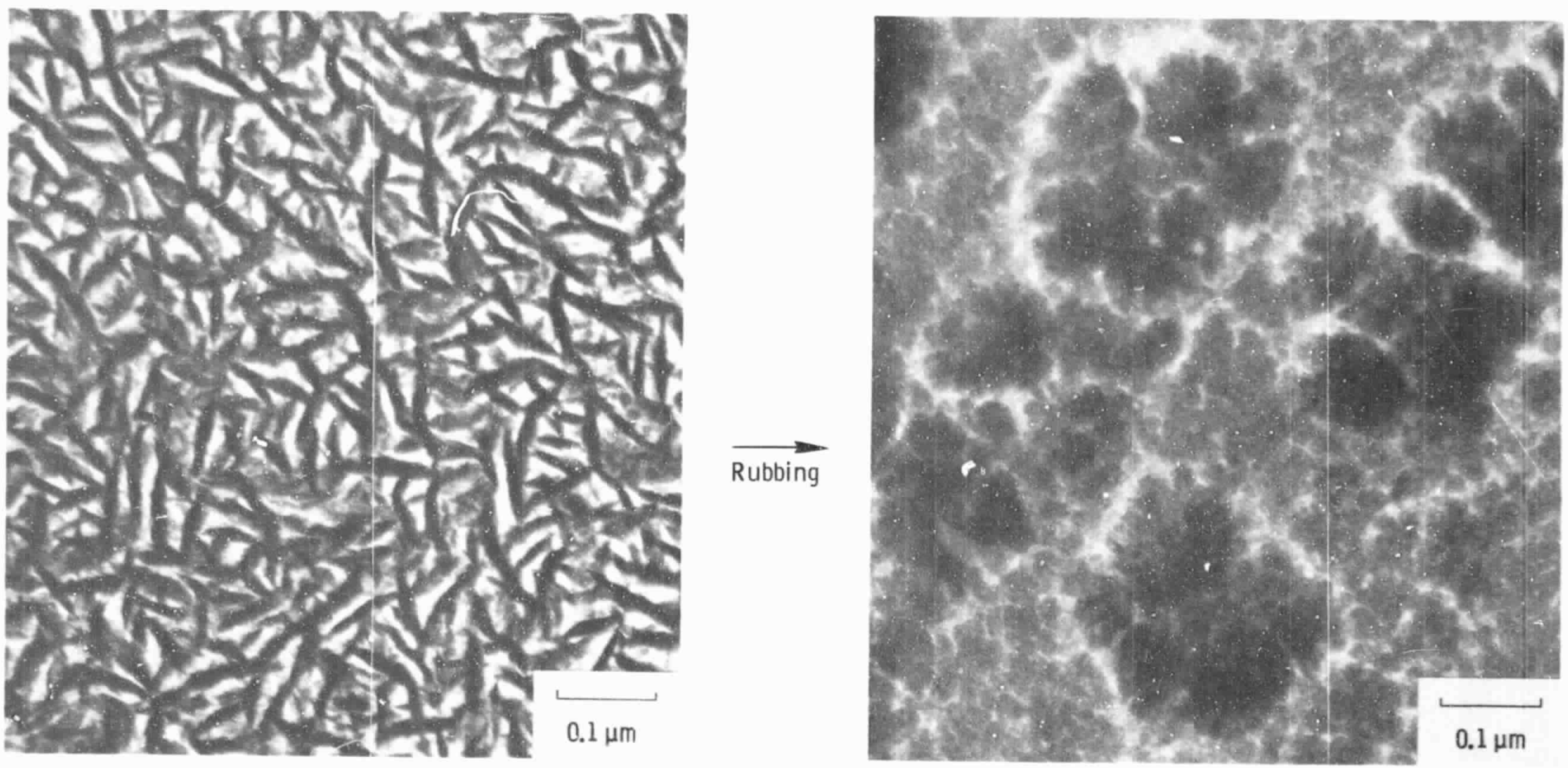

AS-SPUTTERED

AFTER RUBBING

Figure 4. - Transmission electron micrographs of sputtered MoS_2 films.

ORIGINAL PAGE IS
OF POOR QUALITY

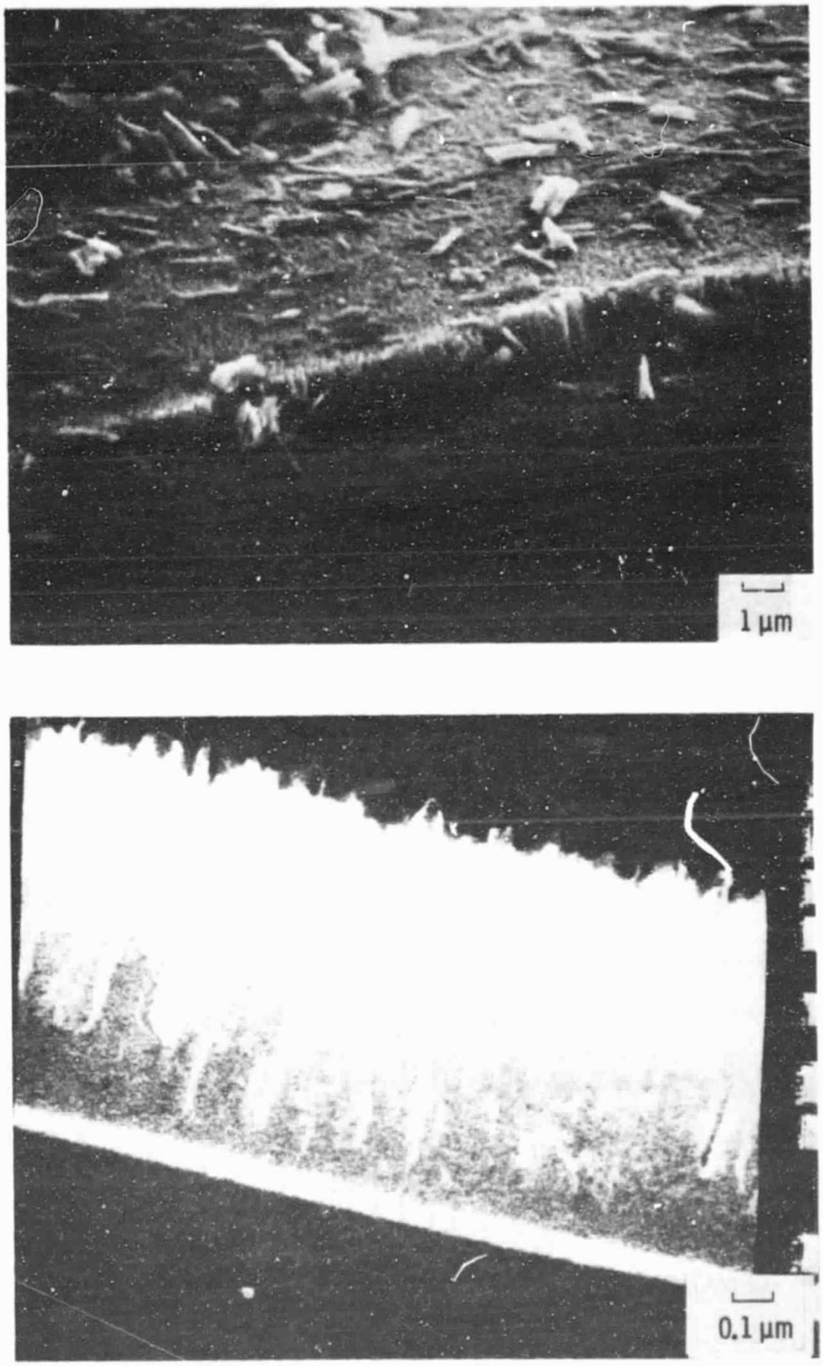

Figure 5. - Cross-sectional structure of sputtered MoS_2 film on glass.

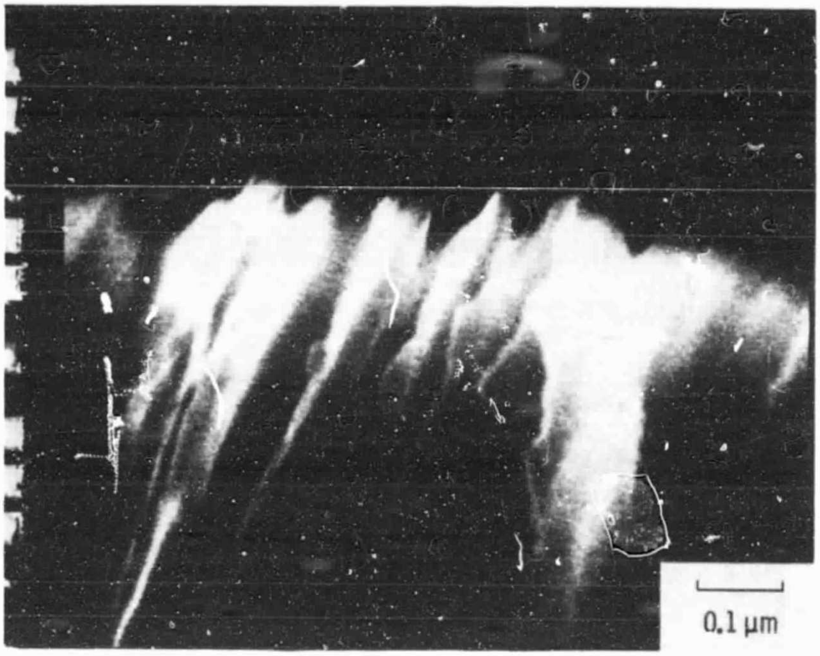

Figure 5. - Concluded.

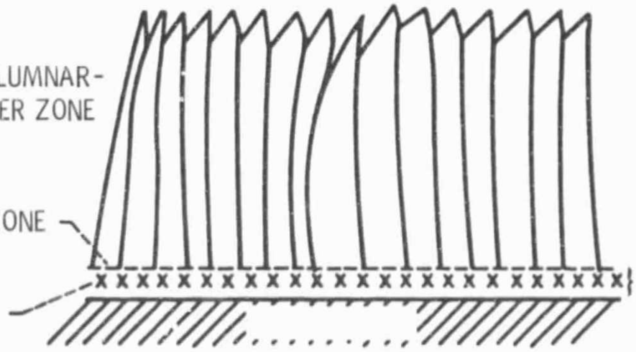

Figure 6. - Morphological growth zones of sputtered MoS_2 films.

ORIGINAL PAGE IS
OF POOR QUALITY

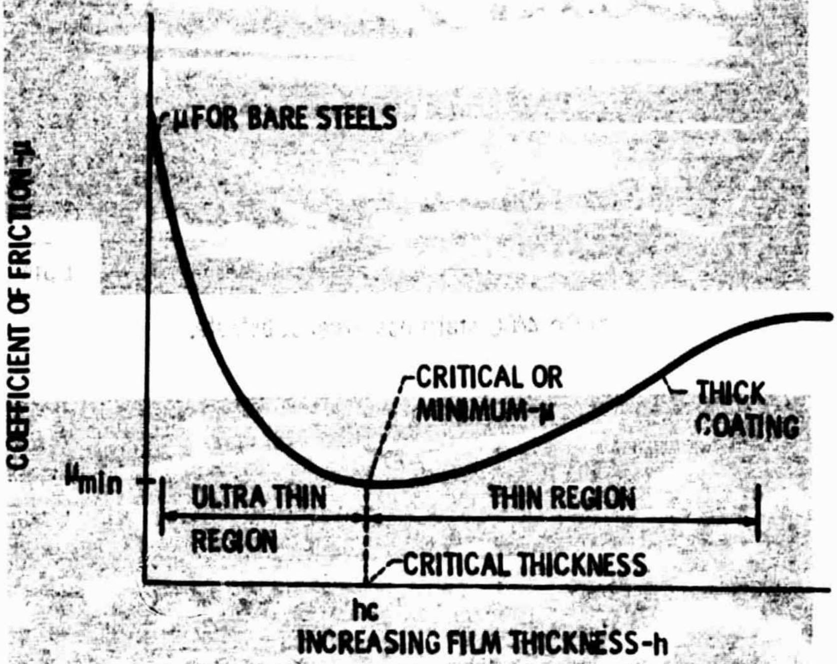

Figure 7. - Schematic representation of the effect of film thickness on the friction coefficient of low shear strength metallic films on steel.

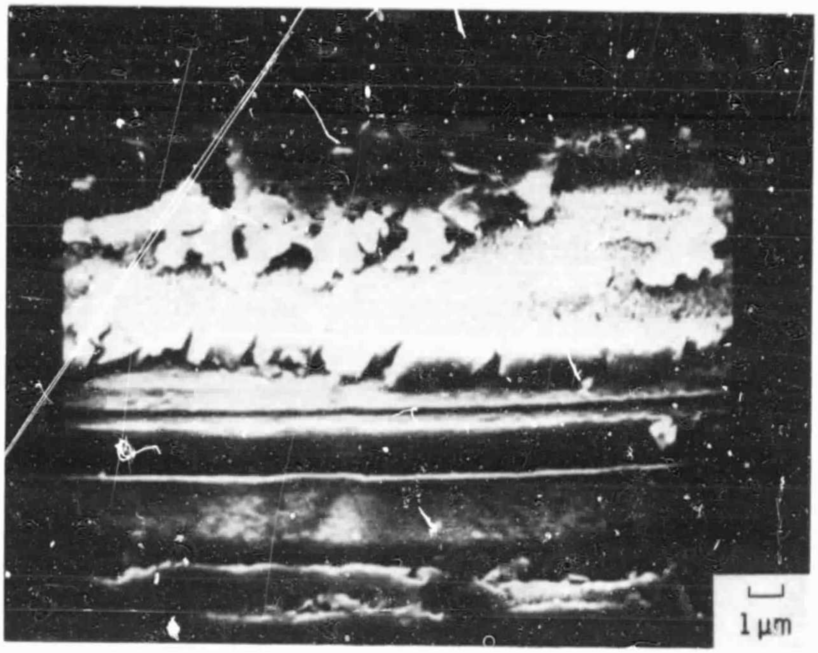

(a) On 440C stainless-steel substrate.

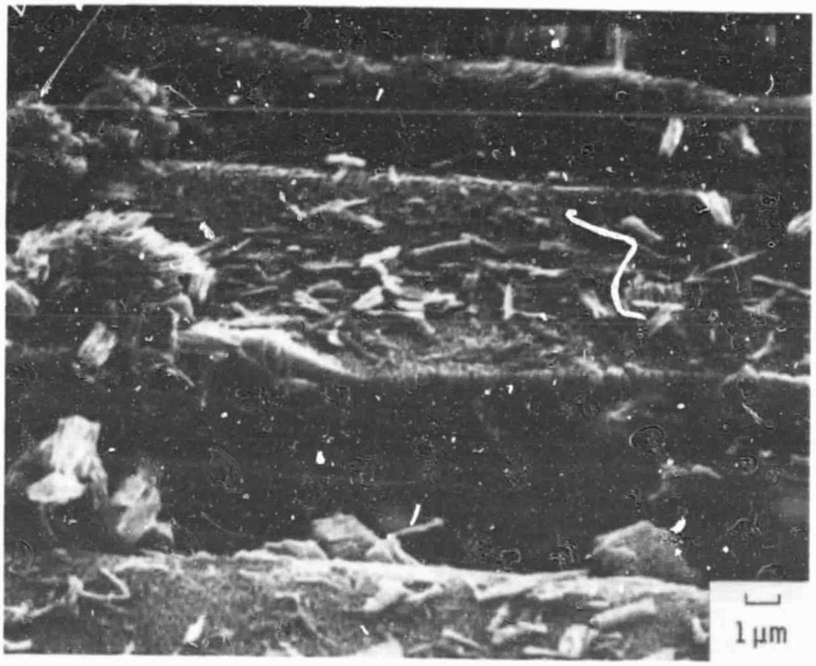

(b) On glass substrate.

Figure 8. - Sputtered MoS_2 film after a single-pass sliding.

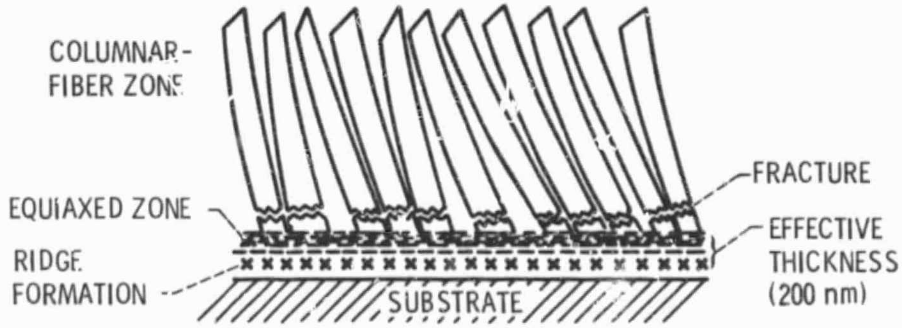

Figure 9. - Fracture during sliding of sputtered MoS_2 film in respect to morphological zones.

ORIGINAL PAGE IS
OF POOR QUALITY

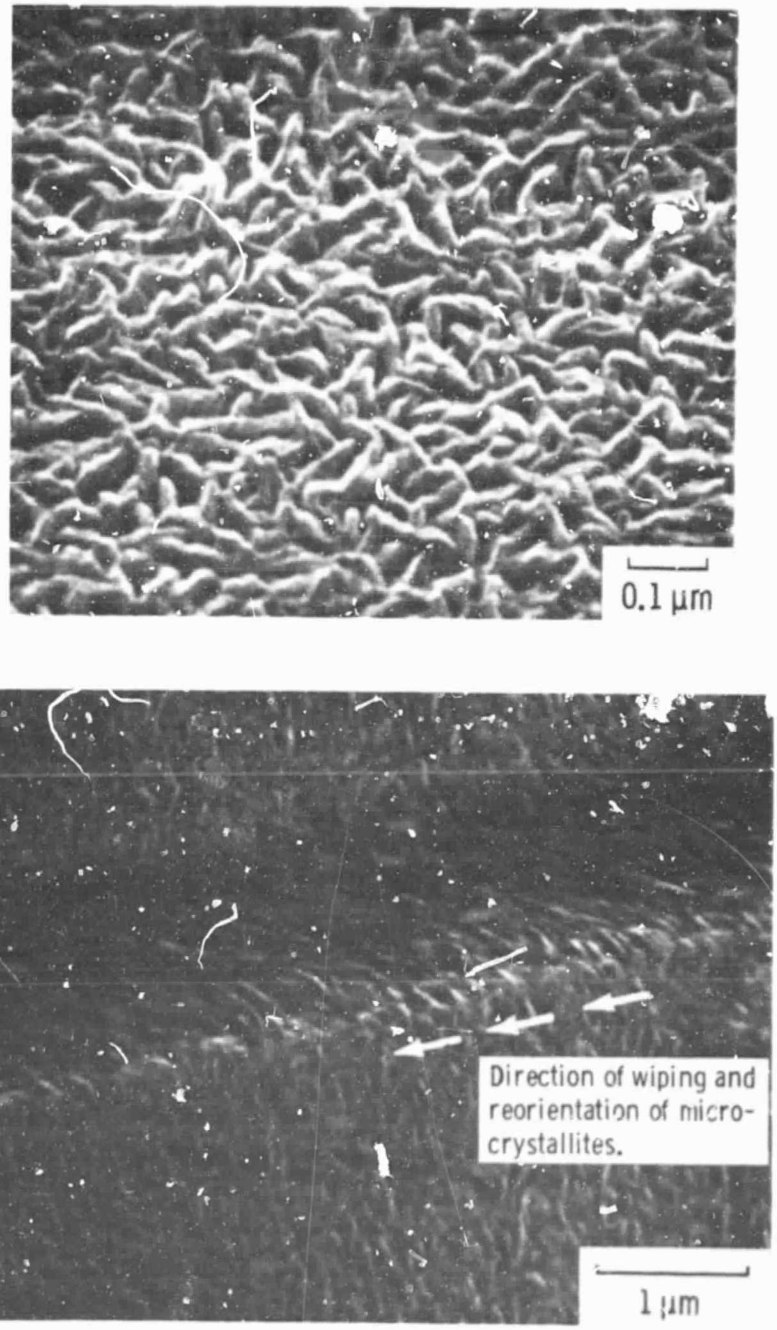

Figure 10. - Surface morphology of microcrystallites before and after wiping and rubbing.

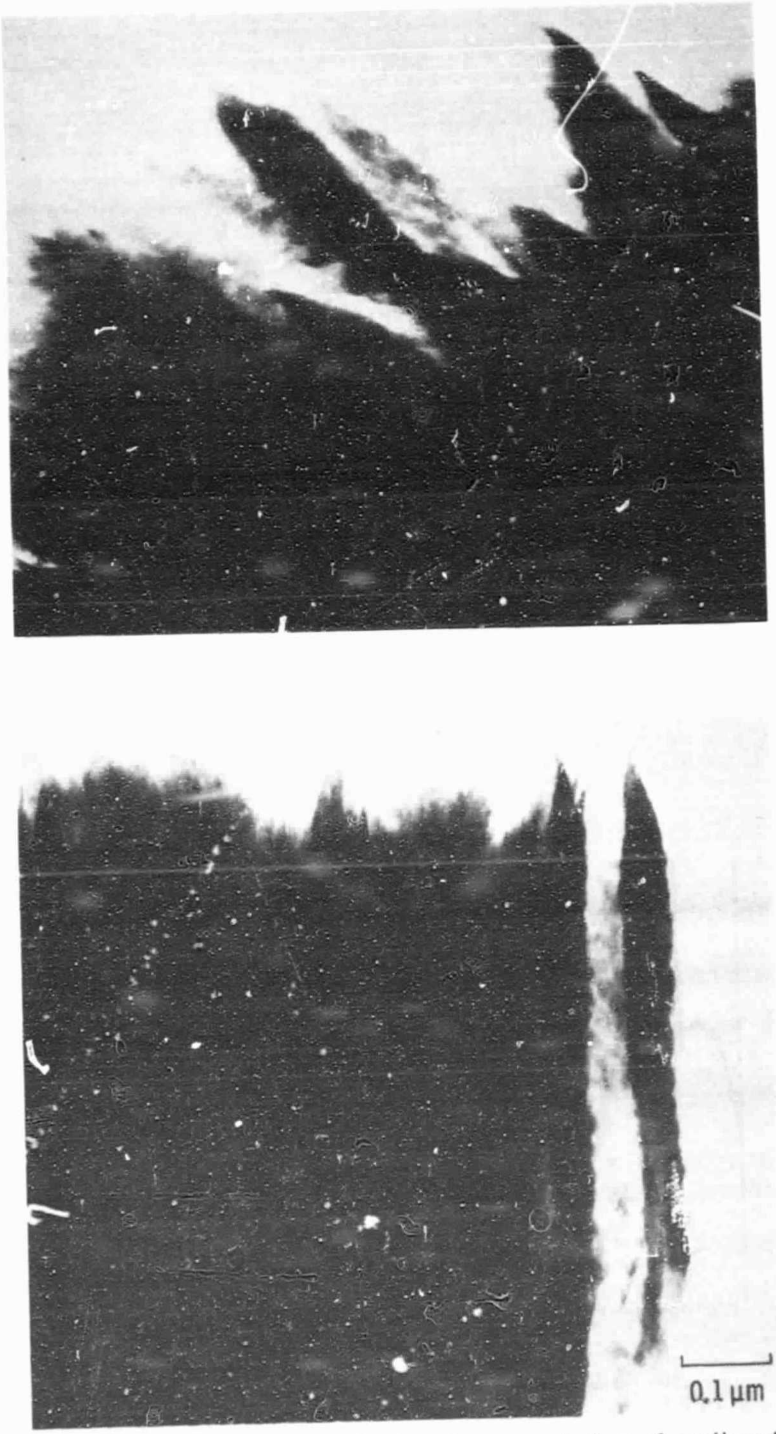

Figure 11. - TEM micrograph of surface morphology of sputtered MoS_2 film.

ORIGINAL PAGE IS
OF POOR QUALITY

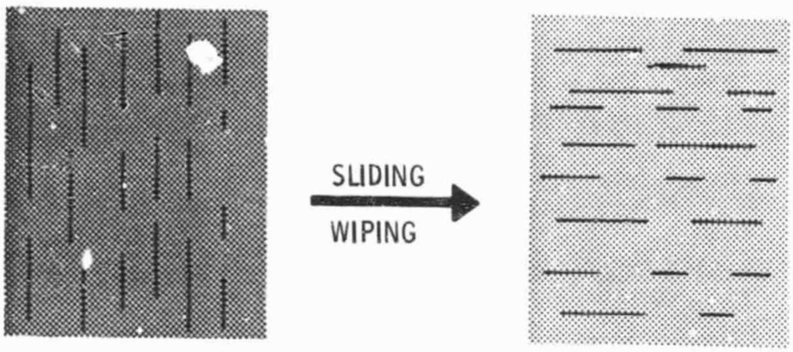

Figure 12. - Reorientation of sputtered MoS_2 platelets.

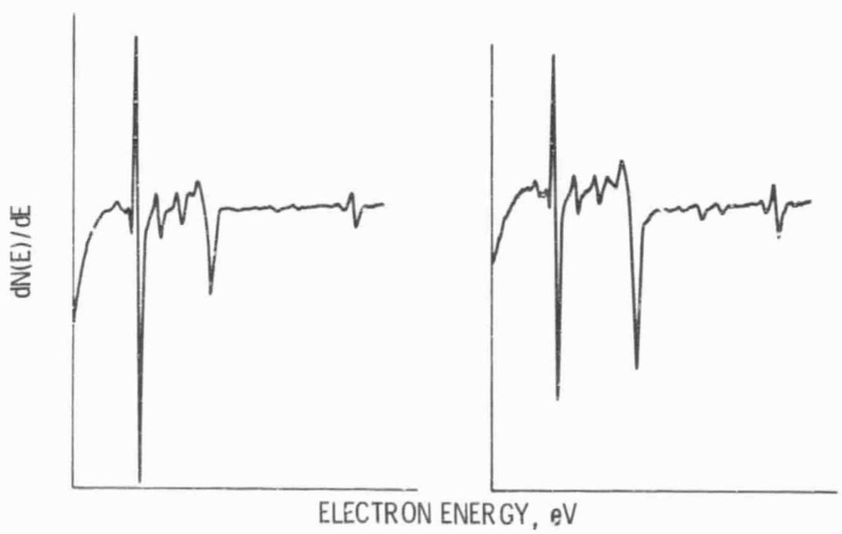

(a) As sputtered. (b) After wiping.

Figure 13. - Auger spectra of sputtered MoS_2 films.